bioRxiv preprint doi: https://doi.org/10.1101/336990; this version posted July 9, 2019. The copyright holder for this preprint (which was not certified by peer review) is the author/funder. All rights reserved. No reuse allowed without permission.

TGFβ blocks IFNα/β release and tumor rejection in spontaneous mammary tumors

Marion V. Guerin[1,2,3], Fabienne Regnier[1,2,3], Vincent Feuillet[1, 2, 3], Lene Vimeux[1,2,3], Julia M. Weiss[1,2,3,$], Georges Bismuth[1,2,3], Gregoire Altan-Bonnet[4], Thomas Guilbert[1,2,3], Maxime Thoreau[1,2,3], Veronica Finisguerra[5], Emmanuel Donnadieu [1,2, 3], Alain Trautmann[1,2, 3*] and Nadège Bercovici[1,2, 3*]

[1]Inserm, U1016, Institut Cochin, Paris, France

[2]Cnrs, UMR8104, Paris, France

[3]Université Paris Descartes, Sorbonne Paris Cité, France.

[4]Cancer & Inflammation Program, National Cancer Institute, Bethesda MD USA

[5]Ludwig Institute for Cancer Research, Brussels, Belgium

*These authors contributed equally to this work

Lead contact: nadege.bercovici@inserm.fr; Phone +33680527946; Fax +33140516555; Institut Cochin, 22 rue Méchain, 75014 Paris

[$]Current address: *Division of Pediatric Hematology and Oncology, University Medical Center, Freiburg, Germany*

Key words: STING; tumor regression; type I Interferon; myeloid cells; TGFβ

Abbreviations: DMXAA: 5,6-dimethylxanthenone-4-acetic acid; IFN: interferon; IRF3: Interferon regulatory factor 3; IRF7: Interferon regulatory factor 7; MHCII : Major histocompatibility complex II; MMTV: Mouse mammary tumor virus; NF-κB: nuclear factor kappa-light-chain-enhancer of activated

bioRxiv preprint doi: https://doi.org/10.1101/336990; this version posted July 9, 2019. The copyright holder for this preprint (which was not certified by peer review) is the author/funder. All rights reserved. No reuse allowed without permission.

B cells; PyMT: polyomavirus middle T antigen; STING: Stimulator of interferon genes; TAM: tumor-associated macrophages; TBK1: TANK-binding kinase 1; TGFβ: tumor growth factor beta; TNFα: Tumor necrosis factor alpha.

bioRxiv preprint doi: https://doi.org/10.1101/336990; this version posted July 9, 2019. The copyright holder for this preprint (which was not certified by peer review) is the author/funder. All rights reserved. No reuse allowed without permission.

Summary

Type I interferons (IFN) are being rediscovered as potent anti-tumoral agents. Activation of the STimulator of INterferon Genes (STING) by DMXAA can induce a strong production of IFNα/β and the rejection of transplanted primary tumors. In the present study, we addressed whether targeting STING with DMXAA also leads to the regression of spontaneous MMTV-PyMT mammary tumors. We show that these tumors are refractory to DMXAA-induced regression. This is due to a blockade in the phosphorylation of IRF3 and the ensuing IFNα/β production. Mechanistically, we identified TGFβ abundant in spontaneous tumors, as a key molecule limiting this IFN-induced-tumor regression by DMXAA. Finally, blocking TGFβ restores the production of IFNα by activated MHCII^{+} tumor-associated macrophages, and enables tumor regression induced by STING activation. On the basis of these findings, we propose that type I IFN-dependent cancer therapies could be greatly improved by combinations including the blockade of TGFβ.

bioRxiv preprint doi: https://doi.org/10.1101/336990; this version posted July 9, 2019. The copyright holder for this preprint (which was not certified by peer review) is the author/funder. All rights reserved. No reuse allowed without permission.

INTRODUCTION

Type I interferon (IFN) α and β are cytokines with a great potential in anti-tumor immunity. It has been shown that endogenous type I IFN constitutes a first line of defense by innate cells, promoting an adaptive immune response not only against viruses but also against cancer cells [1–3]. In fact, modulation of immune responses by type I IFN may occur in several different ways. It often involves the regulation of cytokines and chemokines (CXCL10, CCL3, CCL2, IL-15), which are able to promote the recruitment, survival and activation of various immune cell subsets, including monocytes, dendritic cells (DC), T cells and NK cells. Moreover, IFNα induces the upregulation of MHC I and the acceleration of DC differentiation, thus improving the priming of T cells [4,5]. In addition, the potential of IFNα/β to inhibit protein translation can trigger conflicting signals leading to the death of highly proliferating cancer or endothelial cells [6,7].

Long recognized as a broad immune modulator, type I IFN has been administered for years to treat cancer patients [8]. However, due to its toxicity after systemic administration, it is no longer commonly used as such. A better understanding of the mechanisms by which type I IFN modulates immune responses has renewed the interest for its use. Recently, the ER-associated molecule STING has been the focus of several investigations aiming at restimulating the production of type I IFN in the tumor ecosystem. STING is ubiquitously expressed and is activated by cytosolic nucleotides derived from pathogens or following cellular damages. In particular, it has been shown that STING can sense endogenous cytosolic DNA and contribute to anti-tumor immunity [9]. In particular, synthetic cyclic dinucleotides (CDN) injected intratumorally have been shown to rapidly elicit the expression of IFNβ by endothelial cells in tumors, followed by the generation of anti-tumor specific $CD8^+$ T cells and the regression of transplanted tumors [10,11]. DMXAA (5,6-dimethylxanthenone-4-acetic acid) has the dual property of activating STING and disrupting specifically the tumor vasculature [12]. One intraperitoneal (i.p.) injection is sufficient to induce the regression of primary transplanted tumors, as a single agent or in combination with vaccination [13–15]. In line with this, we have recently reported that the DMXAA

bioRxiv preprint doi: https://doi.org/10.1101/336990; this version posted July 9, 2019. The copyright holder for this preprint (which was not certified by peer review) is the author/funder. All rights reserved. No reuse allowed without permission.

induced-regression of PyMT transplanted tumors relies on IFNα/β production and on the cooperation of T cells with myeloid cells at the tumor site [16].

Together, these reports suggest that inducing type I IFN in solid tumors by targeting the STING pathway is a promising therapeutic approach. Nevertheless, what is unknown is whether it would be sufficient to induce the rejection of solid tumors that arise spontaneously, since multiple resistance mechanisms take place during the progression of spontaneous tumors. In particular, the transplantation of tumor cells induces an acute inflammation locally associated with cell death and priming of the immune cell infiltrate [17]. In contrast, spontaneous tumors emerge from a sterile microenvironment progressively exposed to a chronic inflammation likely to condition differently the immune cell infiltrate. When spontaneous tumors develop in an animal, the T cell repertoire shaped in the thymus and the periphery gives rise to low affinity and anergic tumor-infiltrating T cells [18]. In addition, soluble factors of chronic inflammation like TGFβ are known to suppress various immune effector cells, modulate the profile of myeloid cells and promote the emergence of regulatory T cells. Thus, although transplanted tumors share some elements of immune suppressive environments, their rapid development, within days or weeks, do not integrate the various changes that occur in spontaneous tumors during months of development. In the MMTV-PyMT tumor model, Ming Li and colleagues have described the progressive accumulation of suppressive tumor-associated macrophages (TAM) subsets in the mammary tumors from 8 week-to 20 week-old transgenic mice [19]. The density of such TAM, assimilated to “M2-like macrophages”, which represent a major component of the tumor microenvironment, has been correlated with a poor prognosis in various cancer types in humans [20]. By contrast, detailed analyses of the myeloid cell compartment in human tumors revealed that the density of TAM with an M1-like phenotype correlates with a favorable prognosis in some cancers [21]. In line with this, when appropriately stimulated for instance in the presence of IFN type I, macrophages can mediate anti-tumor activity together with anti-tumor $CD8^+$ T

bioRxiv preprint doi: https://doi.org/10.1101/336990; this version posted July 9, 2019. The copyright holder for this preprint (which was not certified by peer review) is the author/funder. All rights reserved. No reuse allowed without permission.

cells, at least in transplanted tumor models [16,22–26]. Thus, the nature and the activation status of the tumor microenvironment may drastically influence the outcome of therapeutic treatments.

In the present study, we addressed whether targeting STING with DMXAA can induce the regression of spontaneous MMTV-PyMT mammary tumors. We identified TGFβ as a key element that impairs the production of IFN type I by TAM, preventing the induction of tumor regression.

RESULTS

Limited efficacy of DMXAA in the spontaneous MMTV-PyMT mice

To assess if tumors developing in MMTV-PyMT mice (Spont-PyMT) could regress after DMXAA treatment, as reported earlier for transplanted PyMT mice (Trans-PyMT) [16], Spont-PyMT mice were injected intraperitoneally (i.p.) with DMXAA when posterior tumors reached ~ 6 mm in diameter (in approximately 2 month-old mice). For each treated mouse, the size of 8-10 tumors was measured over time. Figure 1a provides an example of the follow up obtained in one Spont-PyMT mouse treated with DMXAA. In the central panel, the raw data (one *tumor* per curve) illustrate the evolution of the tumor size for one mouse. In the right panel of Fig 1a are shown the same data, but the size of each tumor is expressed relative to its size at day 0. This representation allows one to distinguish easily tumors that responded or not to DMXAA treatment. Fig1b illustrates the global follow up obtained in the groups of DMXAA or DMSO treated mice. Overall, DMXAA only slowed down tumor growth compared to control mice, and five days after the DMXAA injection, very few mice (14%) showed regressing tumors in Spont-PyMT mice whereas 95% did in transplanted PyMT (Fig. 1c).

One explanation for this phenomenon could have been that DMXAA could not access Spont-PyMT tumors as it does in Trans-PyMT ones, due to putative differences in the vasculature of Spont-PyMT tumors and of Trans-PyMT ones. To bypass such a potential problem, we assessed if two different

bioRxiv preprint doi: https://doi.org/10.1101/336990; this version posted July 9, 2019. The copyright holder for this preprint (which was not certified by peer review) is the author/funder. All rights reserved. No reuse allowed without permission.

STING ligands, DMXAA or ML RR-S2 CDA could induce the activation of the type I IFN pathway when the drug was injected directly into the tumor. The results obtained after i.t. injections confirmed those obtained after DMXAA i.p. Indeed, both i.t. STING agonists failed to induce tumor regression in Spont-PyMT mice, in sharp contrast with what was observed in the transplanted model (Fig. 1d).

To understand why DMXAA was poorly efficient in these Spont-PyMT mice, we examined the immune response triggered by DMXAA in Spont-PyMT tumors, compared to Trans-PyMT ones. The proportion of $CD45^+$ immune cells infiltrating Spont-PyMT tumors was modestly increased after DMXAA injection (from 35% to 50% of viable cells, Fig. 2a). This was in sharp contrast with the massive infiltration measured in the Trans-PyMT tumors after DMXAA (from 22% to 86% of viable cells). By analyzing the immune cell subsets in more details, we observed a transient neutrophil ($CD11b^+$ $Ly6G^+$) infiltrate at 24h after DMXAA injection (35-40% of the infiltrating cells) in both models. However, the population of TAM ($CD11b^+$ $Ly6C^{neg}$ $Ly6G^{neg}$ $F4/80^+$) persisted in spontaneous tumors after the injection of DMXAA whereas it decreased rapidly in Trans-PyMT tumors (Fig. 2b). In addition, the monocytes ($CD11b^+$ $Ly6C^{high}$ $Ly6G^{neg}$ $F4/80^{lo}$) and CD8 T cell infiltrates remained respectively 2 times and 5 times smaller in Spont-PyMT tumors compared to Trans-PyMT.

Altogether, these data indicated that DMXAA injection in Spont-PyMT tumors induced the recruitment of few immune cells, and had a much smaller impact on tumor regression than in the transplanted tumor model.

Type I IFN production is not induced in Spont-PyMT tumors

As DMXAA induced a weak immune response in Spont-PyMT mice, we measured the cytokines and chemokines expressed in the tumors of treated mice. DMXAA is known to activate the ubiquitous adaptor STING and subsequently triggers the production of TNFα, IFNα/β and chemokines through NFκB, the phosphorylation of IRF3 (pIRF3) and STAT6, respectively [27,28]. Thus, we measured at the

bioRxiv preprint doi: https://doi.org/10.1101/336990; this version posted July 9, 2019. The copyright holder for this preprint (which was not certified by peer review) is the author/funder. All rights reserved. No reuse allowed without permission.

mRNA level the cytokines expressed in the tumor microenvironment shortly after DMXAA injection in Spont-PyMT mice. As shown in Fig. 3a, the transcription of *Tnfα*, *Ccl2*, *Cxcl1* and *Ccl20* was upregulated in Spont-PyMT tumors, like in Trans-PyMT ones (Fig. S1a), even though the fold increases were not always similar in the two tumor types. Strikingly, no significant increase in mRNA levels of *Ifnα* and *Ifnβ* genes was detected in the spontaneous tumor model (Fig. 3a) whereas these genes were highly expressed from 3h to 24h after DMXAA treatment in transplanted tumors (Fig. S1a). The absence of type I IFN transcripts in DMXAA-treated spontaneous tumors was confirmed at the protein level when Spont-PyMT tumor cell suspensions were stimulated *in vitro* with DMXAA, in sharp contrast to Trans-PyMT ones (Fig. S1b).

We tested if this lack of type I IFN production after DMXAA injection in the spontaneous PyMT mice was DMXAA-specific. To this aim, we used another STING agonist, the CDN 2'3' cGAMP drug. The intra-tumoral injection of CDN 2'3' cGAMP also failed to induce the upregulation of *Ifnα* or *Ifnβ* genes in Spont-PyMT tumors, whereas it did in Trans-PyMT tumors (Fig. 3b). Moreover, the TLR4 ligand LPS, another inducer of type I IFN, induced *Ifnα* , *Ifnβ* and *Tnfα* mRNA levels within 3 hours in Trans-PyMT tumors, while only *Tnfα* was upregulated by LPS in Spont-PyMT tumors (Fig. 3c).

Taken together, these data show that Spont-PyMT mice have an intrinsic defect in the production of type I IFN in response to STING or TLR4 stimulation, which may explain their resistance to DMXAA treatment.

DMXAA fails to induce the phosphorylation of IRF3 in Spont-PyMT tumors

To identify at which molecular level the induction of type I IFN expression was blocked, we next analyzed the early signaling molecules involved in the STING activation pathway. The phosphorylation of IRF3 (pIRF3) is necessary for type I IFN production. We first measured pIRF3 by immunofluorescence in tumor slices from transplanted and spontaneous tumors, as soon as 3h after

bioRxiv preprint doi: https://doi.org/10.1101/336990; this version posted July 9, 2019. The copyright holder for this preprint (which was not certified by peer review) is the author/funder. All rights reserved. No reuse allowed without permission.

DMXAA injection. A strong pIRF3 labeling was detected after DMXAA treatment in slices of Trans-PyMT tumors (Fig. 4a, right panel) including in myeloid cells (F4/80$^+$) and some endothelial (CD31$^+$) cells (Fig. 4b). By contrast, pIRF3$^+$ cells were hardly detectable in tumor slices of DMXAA-treated Spont-PyMT tumors (Fig. 4a, left panel). Similar results were obtained after intratumoral injection DMXAA or ML RR-S2 CDA (Fig. S3). These results indicate that DMXAA injection failed to activate the IFN pathway in any cell type of the tumor ecosystem in Spont-PyMT mice, due to a blunted pIRF3 level. We verified that there was no difference in *Sting, Irf3 and Irf7* intratumoral mRNA transcripts between Spont- and Trans-PyMT mice (Fig. S2a). In addition, the Tank binding kinase 1 (TBK1), which is responsible for the phosphorylation of IRF3, was phosphorylated in both tumor models after DMXAA treatment (Fig. S2b). These results are consistent with the upregulation of *Tnfα* and chemokines mRNA levels after DMXAA injection (Fig. 3a) and indicates that the signaling pathway leading to type I IFN production is altered downstream of TBK1 activation.

Taken together, these results indicate that, although the two models were based on the same tumor cells, the tumor microenvironment of spontaneous Spont-PyMT mice is resistant to the induction of type I IFN production. This defect is likely due to the blockade of IRF3 phosphorylation.

Anti-TGFβ unlocks type I IFN production by macrophages in tumors of Spont-PyMT mice

TGFβ is frequently accumulated in tumors where it is known to inhibit the production of pro-inflammatory cytokines by macrophages, including IFNβ [29]. Therefore, we examined if TGFβ was involved in the impaired type I IFN production following DMXAA administration to Spont-PyMT mice. Strikingly, TGFβ mRNA was expressed at much higher levels (~7 fold) in untreated Spont-PyMT tumors than in Trans-PyMT ones (Fig. 5a). In addition, as shown in Figure 5b, the vast majority of cells in spontaneous tumors, and not in transplanted ones, showed nuclear pSmad2/3 expression,

bioRxiv preprint doi: https://doi.org/10.1101/336990; this version posted July 9, 2019. The copyright holder for this preprint (which was not certified by peer review) is the author/funder. All rights reserved. No reuse allowed without permission.

indicating active signaling through TGFβR in these tumors. Nuclear pSmad2/3 was found in F4/80$^+$ myeloid cells, gp38$^+$ fibroblasts and EpCAM$^+$ tumor cells (Fig. 5c).

We thus wondered if an anti-TGFβ treatment could render Spont-PyMT mice more sensitive to DMXAA. To test this, Spont-PyMT mice were treated with an anti-TGFβ antibody for 4 days then injected with DMXAA, sacrificed 3h later and the phosphorylation of IRF3 was measured in tumor slices. As shown in Figure 6a, the pretreatment of mice with an anti-TGFβ *in vivo* allowed DMXAA to induce the phosphorylation of IRF3 in a fraction of cells. This is in contrast with the total absence of DMXAA-induced pIRF3 when Spont-PyMT are not treated with anti-TGFβ, as shown in Figure 4a. Among the pIRF3$^+$ cells, both F4/80$^+$ myeloid cells and tumor cells were identified (Fig. S4a). Moreover, this anti-TGFβ neutralization unleashed the expression of *Ifnα* and *Ifnβ* genes after DMXAA injection in Spont-PyMT treated mice (Fig. S4b). Similar results were obtained at the protein level when tumor cell suspensions from anti-TGFβ treated Spont-PyMT mice were stimulated with DMXAA in vitro (Fig. S4c).

To check the importance of myeloid cells in the initial DMXAA-induced burst of inflammatory cytokines [16,30], we depleted these cells *in vivo* before DMXAA injection. This experiment demonstrates that myeloid cells were indeed responsible for type I IFN expression (Fig. S4b). We further analyzed the proportion and phenotype of myeloid cells infiltrating the anti-TGFβ treated Spont-PyMT tumors. There was no quantitative difference in terms of cell proportions between anti-TGFβ treated and untreated Spont-PyMT tumors. In both cases, TAM was the main myeloid cell population of the immune infiltrate (Fig. S4d). However, there was a qualitative difference in these cells. Indeed, TGFβ blockade was accompanied by a doubling in activated MHCII$^+$ TAM compared to untreated mice, reaching frequencies comparable to those observed in Trans-PyMT tumors (Fig. 6b). The few infiltrating monocytes were also mainly MHC II$^+$ in anti-TGFβ-treated mice as in Trans-PyMT. Finally, we purified the immune cells from anti-TGFβ treated Spont-PyMT tumors and tested if F4/80$^+$ cells were responsible for IFNα production. After *in vitro* stimulation with DMXAA, the F4/80$^+$ cell

bioRxiv preprint doi: https://doi.org/10.1101/336990; this version posted July 9, 2019. The copyright holder for this preprint (which was not certified by peer review) is the author/funder. All rights reserved. No reuse allowed without permission.

fraction produced a much larger amount of IFNα than the F4/80$^-$ fraction (Fig. 6c). Furthermore, when MHCII$^+$ subsets of TAM were sorted and stimulated *in vitro* with DMXAA, they tended to produce more IFNα than their MHC II$^-$ counterpart (Fig. S4e).

Together, these results indicated that TGFβ blockade rendered Spont-PyMT mice more sensitive to DMXAA stimulation by promoting the infiltration of mammary tumors by activated MHC II$^+$ TAM capable of producing type I IFN.

TGFβ inhibits IRF3 phosphorylation and type I IFN production by macrophages

To decipher by which molecular mechanisms TGFβ could interfere with the production of type I IFN in macrophages, we switched to *in vitro* experiments performed with Bone Marrow-Derived Macrophages (BMDM). After one week of differentiation, BMDM were exposed to TGFβ overnight and their capacity to phosphorylate IRF3 in response to DMXAA was evaluated. We found that TGFβ-treated BMDM had strikingly lost their ability to phosphorylate IRF3 when stimulated with DMXAA for 3h (Fig. S5a and b). This was not due to a direct effect of TGFβ on DMXAA-induced signaling since the mere addition of TGFβ together with DMXAA to BMDM that had not been pretreated with TGFβ did not block IRF3 phosphorylation (data not shown).

It has been reported that the Histone Deacetyl Transferase HDAC4 in the cytoplasm can inhibit type I IFN production[31] and that TGFβ can stimulate a ROS-dependent export of HDAC4 out of the nucleus [32]. We thus examined whether TGFβ signaling could also alter the subcellular localization of HDAC4 in macrophages. In BMDM, HDAC4 was mainly nuclear (Fig. S5c). By contrast, exposure of BMDM to TGFβ overnight induced a substantial translocation of the molecule to the cytoplasm, as shown by its homogeneous distribution in these cells. Moreover, the inhibition of ROS production during TGFβ

bioRxiv preprint doi: https://doi.org/10.1101/336990; this version posted July 9, 2019. The copyright holder for this preprint (which was not certified by peer review) is the author/funder. All rights reserved. No reuse allowed without permission.

exposure decreased this translocation of HDAC4 (Fig. S5c) and restored the phosphorylation of IRF3 after DMXAA stimulation (Fig. S5a and b).

Together, these results showed that TGFβ could induce molecular changes in macrophages susceptible to affect their ability to produce type I IFN. We identified ROS-mediated relocalization of HDAC4 as one molecuular mechanism by which TGFβ can specifically interfere with the phosphorylation of IRF3 and thus regulate type I IFN response in these cells.

Blocking TGFβ allows for DMXAA-induced tumor regression in Spont-PyMT mice

We finally wondered if TGFβ blockade could facilitate DMXAA-induced tumor regression in Spont-PyMT mice. Mice were treated with a combination of anti-TGFβ and DMXAA, the latter being injected once i.p., 4 days after the beginning of the anti-TGFβ treatment. In these conditions, the tumor burden of Spont-PyMT mice was diminished (66%) or stabilized (33%) within 5 days following the combined treatment (Fig. 6d). This response was not dependent on CD8 T cells, but required IFN signaling since it was completely blocked in mice treated with an anti-IFNAR antibody. Altogether, these results showed that blocking TGFβ allowed DMXAA-induced type IIFN production by tumor-infiltrating macrophages and facilitated a transient tumor regression in Spont-PyMT mice.

bioRxiv preprint doi: https://doi.org/10.1101/336990; this version posted July 9, 2019. The copyright holder for this preprint (which was not certified by peer review) is the author/funder. All rights reserved. No reuse allowed without permission.

Discussion

Type I IFN have the unique potential to promote the activation and recruitment of various immune effectors and represent a natural defense, mainly against viruses. IFN can also help to fight cancer and encouraging results have already been obtained in transplanted tumor models with STING ligands, able to trigger IFN production [10,16]. However, whether one can induce the production of type I IFN therapeutically in spontaneous tumors remains a burning issue. Here, we provide an example in which TGFβ accumulation in the microenvironment of spontaneous tumors prevents the production of IFNβ/α by macrophages after STING activation and contributes to prevent tumor rejection. This obstacle can be overcome with an anti-TGFβ treatment.

Truncated activation of the STING/TBK1/IRF3 pathway compromises regression of Spont-*PyMT tumors*

In sharp contrast with the tumor regression systematically induced by DMXAA in transplanted PyMT mice [16], we report here that Spont-PyMT tumors rarely regress after STING activation. A weak immune response was associated with the failure of DMXAA-induced tumor regression. What was specifically lacking in spontaneous tumors was the production of IFNβ and IFNα, not the production of immune-attractant chemokines. Four distinct type I IFN inducers (DMXAA, LPS, cGAMP and ML RR-S2 CDA) failed to induce the production of IFNβ/α in these spontaneous tumors. These results suggest that spontaneous tumors develop some particular features that inhibit the induction of an IFN-dependent anti-tumor immunity, a hypothesis which prompted us to study the activation of this pathway in the Spont-PyMT tumor model.

We found that the absence of type I IFN mRNA after DMXAA injection in Spont-PyMT mice was associated with a dramatic defect in IRF3 phosphorylation in the tumor ecosystem, both in tumor cells and in immune infiltrating cells. On the contrary, the activation of TBK1, necessary for the

bioRxiv preprint doi: https://doi.org/10.1101/336990; this version posted July 9, 2019. The copyright holder for this preprint (which was not certified by peer review) is the author/funder. All rights reserved. No reuse allowed without permission.

activation of IRF3, was preserved, indicating a specific block downstream of the STING/TBK1 pathway. The transcription of the *Ifn*β gene, which is known to be driven by pIRF3 homodimers or by pIRF3/pIRF7 heterodimers, was thus likely blocked at an early stage. A positive feedback loop mediated by IFNAR signaling normally allows further upregulation of *Irf7* mRNA and IFNα production. As expected, no upregulation of *Irf7* gene expression took place in Spont-PyMT tumors after DMXAA compared to Trans-PyMT tumors (data not shown), probably as a direct consequence of the absence of pIRF3 and IFNβ.

Decreased responsiveness to IFNα has already been reported in cancer patients [33], with reduced phosphorylation of STAT1 after stimulation with IFNα *in vitro*. Our study adds a key element: the capacity to produce IFNβ and IFNα may also be compromised in some tumors. This finding highlights that a defect in IFNβ/α production in a tumor may originate from an early block in STING/IRF3 signaling. This adds up to the well-known defective IFNα production by some tumor cells, which may result from mutations or epigenetic regulation of this pathway [34,35], and which provides an advantage for therapeutic interventions with oncoviruses [35]. Here, the therapeutic potential of STING agonists to boost an anti-tumor response in solid tumors relies on the capacity of the tumor microenvironment to produce type I IFN. The Spont-PyMT mammary model illustrates that some tumors may be resistant to such interventions.

Our data further suggest that following DMXAA treatment, it is the tumor microenvironment that chiefly governed the IFNβ/α production. Thus, endothelial cells and a large fraction of myeloid cells in Trans-PyMT tumors, strongly phosphorylated IRF3 following DMXAA injection. These results are consistent with earlier reports by Demaria and colleagues showing that endothelial cells rapidly produce IFNβ following injection of STING agonist[11]. Note however that in our experiments, endothelial cells were unlikely to be the main source of type I IFN as suggested in Demaria's work, but represented only a minute fraction of pIRF3^{+} cells, susceptible to produce IFNβ. It should also be underlined that tumor cells did not produce IFNα *in vitro* (data not shown), which hints at the

bioRxiv preprint doi: https://doi.org/10.1101/336990; this version posted July 9, 2019. The copyright holder for this preprint (which was not certified by peer review) is the author/funder. All rights reserved. No reuse allowed without permission.

existence of an additional checkpoint between pIRF3 and IFNα production. Together, our data therefore suggest that the different abilities of Trans- and Spont-PyMT to produce type I IFN resides in different tumor microenvironment, essentially in myeloid cells.

TGFβ impairs IFNβ/α production in the tumor microenvironment of Spont-PyMT mice

We found that an anti-TGFβ treatment allowed DMXAA to induce the activation of IRF3, the production of IFNα, and to facilitate tumor regression in Spont-PyMT mice. TGFβ is fundamental in many physiological functions, including the regulation of mammary gland development. Although it may inhibit cell proliferation (and therefore, initial tumor growth), TGFβ is better known for its negative role later on. Indeed, it suppresses immune effector functions, accelerates metastasis dissemination [36], and this effect is amplified by the frequent mutations in the TGFβR signaling pathway allowing tumor cells to escape TGFβ anti-proliferative effect. Not surprisingly, high levels of the active form of TGFβ have been associated with poor survival in several advanced cancers[37]. Of particular interest, the density of pSmad2/3 in the stroma, downstream TGFβR signaling, has been associated with poor prognosis in non-small cell lung cancer [38]. In Spont-PyMT mice, the *Tgfβ* mRNA level was high and nuclear pSmad2/3 was observed in the vast majority of cells of the tumor ecosystem, indicating that the cellular source of TGFβ is unlikely to be unique. We have not attempted to identify the source of TGFβ, but it is well known that it may be secreted by multiple cell types, including macrophages [39] and apoptotic cells [40]. Such signs of massive TGFβ signaling were never observed in Trans-PyMT tumors.

We consider likely that in Spont-PyMT mice, and probably other spontaneous tumors, a major mode of action of TGFβ is indirect. Indeed, it has been shown that TGFβR signaling is involved in the suppression of pro-inflammatory cytokines and the polarization of myeloid cells [29]. Our study provides new elements for understanding these inhibitory effects. Indeed, we have described a

bioRxiv preprint doi: https://doi.org/10.1101/336990; this version posted July 9, 2019. The copyright holder for this preprint (which was not certified by peer review) is the author/funder. All rights reserved. No reuse allowed without permission.

situation where, following the action of a STING ligand, TBK1 is phosphorylated, but not IRF3. The observation of a TGFβ-induced cytoplasmic relocalization of HDAC4 in BMDM, in a ROS-dependent way, is striking. It is consistent with that previously reported in fibroblasts [32]. HDAC4 could be a key player in TGFβ–induced effects. It has been shown that HDAC4 can exert a negative feed-back loop in IFNβ signaling, by interacting with the TBK1/IKKε complex [31]. Such an HDAC-TBK1 interaction could explain how TGFβ introduced a block between TBK1 and IRF3 phosphorylation. Additional mechanisms may affect the responsiveness of TGFβ-treated macrophages, like an interference by Smad2 and Smad3 that can directly inhibit IRF3, resulting in reduced IFNα/β production [41]. In parallel to these molecular changes, we found that tumors that are sensitive to type I IFN induction, *i.e.*, Trans-PyMT or TGFβ-treated Spont-PyMT, were infiltrated by a majority of MHC II^{+} TAM that produce more type I IFN than the MHC II^{-} TAM, which dominate in Spont-PyMT resistant tumors. In line with this, the presence of TGFβ in triple negative human breast tumors has been associated with the functional weakness of infiltrating plasmacytoid DC for producing type I IFN [42]. Our findings indicate that TGFβ blockade allows the reprogramming of anti-tumoral infiltrating myeloid cells. Similarly, the blockade of TGFβ signaling has been shown to promote the emergence of anti-tumoral neutrophils [43].

Numerous studies have proposed explanations for the protumoral action of TGFβ. Many of them deal with the direct immunosuppressive effect of TGFβ (including their release by regulatory T cells) on T cells [44–46]. Others attribute it to the polarization of myeloid cells towards an immunosuppressive phenotype [29], or to its effect on cancer-associated fibroblasts [47,48], and to the ability of T cells to contact tumor cells, even though the underlying molecular mechanism of inhibition remained elusive. We propose here an additional and novel molecular mechanism by which TGFβ may exert a protumoral effect in spontaneous tumors, through the blunting of IFNα/β production.

bioRxiv preprint doi: https://doi.org/10.1101/336990; this version posted July 9, 2019. The copyright holder for this preprint (which was not certified by peer review) is the author/funder. All rights reserved. No reuse allowed without permission.

Combination therapies with TGFβ blockade

We have shown here that an anti-TGFβ treatment unlocks the production of type I IFN by tumor-infiltrating macrophages in response to DMXAA injected in Spont-PyMT mice. These treated mice are not completely equivalent to the transplanted once, in terms of DMXAA-induced IRF3 phosphorylation and IFNα production and there are obviously other differences between the two tumor models, which have no reason to all be TGFβ-dependent. Nevertheless, this combined treatment allows for a transient regression of the tumor by a mechanism independent of CD8 T cells. It is possible that the release of type I IFN, together with TNFα, has a direct effect on the tumor vasculature and the killing of tumor cells [49]. Tumor-infiltrating-macrophages are known to play an important role in the production of these cytokines, and we have previously proven their implication, together with that of CD8 T cells, in the DMXAA-induced regression of Trans-PyMT tumors [16]. We propose that anti-TGFβ combined with DMXAA treatment in Spont-PyMT mice induced an innate anti-tumor response. Finally, the DMXAA-induced regression of spontaneous tumors after anti-TGFβ is transient, indicating that the initial innate responses would deserve being reinforced and prolonged by a treatment boosting the endogenous adaptive anti-tumor response.

The TGFβ/type I IFN interference highlighted in this study is likely to matter not only for STING agonists under active development, but also for chemotherapeutic agents like anthracyclins, for which tumor regression has been associated with a type I IFN signature [50]. In the case of tumors like breast tumors that poorly respond to anti-PD1/PDL1 checkpoint inhibitors and in which TGFβ and M2-like macrophages are abundant [21,36], there would be a solid rationale for using a triple combination of anti-TGFβ, anti-PD-1 and a third partner, such as STING agonist or chemotherapy.

bioRxiv preprint doi: https://doi.org/10.1101/336990; this version posted July 9, 2019. The copyright holder for this preprint (which was not certified by peer review) is the author/funder. All rights reserved. No reuse allowed without permission.

Experimental procedures

Animal studies

MMTV-PyMT transgenic mice are maintained by backcrossing on FvB/NCrl mice (Charles River laboratories). Transplanted PYMT mice were generated as described in a previous work [16]. Briefly, fresh tumor cell suspensions were prepared from MMTV-PyMT tumor bearing mice by mechanical and enzymatic dissociation and were then injected (10^6 cells) in one mammary gland of FvB mice. Mice were maintained at the Cochin Institute SPF animal facility. Animal care was performed by expert technicians in compliance with the Federation of European Laboratory Animal Science association and under the approval of the animal experimentation ethics committee of Paris Descartes (CEEA 34, 16-063).

Mice with tumors of 6mm in diameter received a single i.p. DMXAA injection (23 mg/kg in DMSO, Sigma) or 100 µl of 50% DMSO in PBS as control. When specified, DMXAA was injected i.t. (500 µg). LPS (1x 50 µg) was injected i.p., cGAMP (InvivoGen, 1 x 25 µg) was injected i.t. and mice were sacrificed 3 hours later. ML RR-S2 CDA (MedChem Express, 3 x 50 µg) was injected i.t. at day0, 3 and 6. For antibody treatment, 200 µg of anti-TGFβ (clone 1D11), anti-IFNAR (clone Mar1-5A3), anti-CD8 (clone 53-6.72) or anti-GR1 (clone RB6-8C5) antibodies, all purchased from Bioxcell, were injected every 2 days from days -3 to day +6 after DMXAA treatment. In some experiments, mice were fed with chow containing PLX3397 or control chow (Plexxikon Inc., from day-2 to day +1), to deplete macrophages. Cell suspensions for *in vitro* experiments or flow cytometry characterization were prepared by mechanical and enzymatic dissociation [16].

The evolutions of tumor size after DMXAA treatment are estimated as follows. For each tumor, its size at time t has been calculated, relative to its size at d0, when DMXAA has been injected. For each mouse, the average was calculated for all its measurable tumors. Another representation of DMXAA-induced changes in tumor size starts with a snapshot of the change in tumor burden at day 5 post-

bioRxiv preprint doi: https://doi.org/10.1101/336990; this version posted July 9, 2019. The copyright holder for this preprint (which was not certified by peer review) is the author/funder. All rights reserved. No reuse allowed without permission.

DMXAA injection, measured as above, and pooled for all the mice of the cohort in 3 groups: global progression of the tumor burden when the increase in a mice is > 20%; global regression if the tumor burden has decreased by > 30%, and stabilization in between.

Multicolor flow cytometry

Tumor cells suspension ($4x10^6$) were stained in 96-wells round bottom plates with live/dead staining (Blue fluorescent reactive dye, Invitrogen) during 20 minutes at room temperature. Fc receptors were blocked with anti-FcR (anti-CD16 CD-32 at 5µg/ml, BD Pharmingen). After 2 washes in PBS 2% FCS, cells were stained with the following antibodies CD45-AF700, CD11b-BV421, Ly6C-APCCy7, Ly6G-BV510, F4.80 BV650, IA/IE-BV785, CD206-PE, CD64-APC, CD11c-PeCy7 (for myeloid and MHC II staining, all used at 1:100), with CD45-AF700, TCRβ-BV605, CD4-BV711 and CD8-PerCPef710 antibodies (for lymphoid staining, all used at 1:100) antibodies, all purchased from BD Pharmingen. After washing in PBS, cells were fixed in 1% PFA, stored at 4°C, and acquired the next day with LSR II flow cytometer (BD Bioscience). For detection of phosphorylated proteins staining, cell suspensions were stimulated 3h with DMXAA 250µg/ml, fixed immediately in PFA 4%, permeabilized with frozen methanol 90%, stained overnight with pIRF3-AF647 (1:10) or pTBK1-PE (1:100) antibodies (both purchased from Ozyme), then washed and analyzed by multicolor flow cytometry.

Differentiation and culture of bone marrow–derived macrophages (BMDM)

Bone marrow cells were collected from FvB mice. With a syringe, the marrow was flush out with a needle of 25G into a sterile Petri dish with DMEM. Then, the cells were centrifuged, resuspended in DMEM supplemented with glutamine, 30% L929 conditioned-medium, 20% FCS and 2% P/S. BMDM were used in experiments after 5 days of culture. BMDM were incubated overnight at 37°C with TGFβ (Peprotech; 5ng/ml), the ROS inhibitor NacetylCysteine (ThermoFicsher; 1nM) or left untreated. Then, cells were stimulated or not with DMXAA (Sigma; 250 µg/ml) during 3 hours.

bioRxiv preprint doi: https://doi.org/10.1101/336990; this version posted July 9, 2019. The copyright holder for this preprint (which was not certified by peer review) is the author/funder. All rights reserved. No reuse allowed without permission.

Imumunofluorescence

Tumor pieces were fixed overnight with Periodate-Lysine-Paraformaldehyde at 4°C. Immunofluorescence on thick tumor slices (350 µm) was performed as previously described [51]. Immunostaining of surface markers was performed at 37°C for 15 min with antibodies specific for EpCAM-BV421, F4/80-AF488 or AF647, Gp38-PEor CD31-PE (all from BD Pharmingen and used at 1:100). For additional intracellular staining, tissue slices were fixed in 4% PFA (10min RT) and permeabilized with methanol 90% 30min at 4°C and stained overnight with p-IRF3-AF647 (1:10) or p-SMAD2/3 (cell signaling used at 1:100). For detection of pSMAD2/3, primary anti-pSMAD2/3 Ab was revealed with anti-rabbit Alexa 488 (life technologies; 1:200).

Images of tumor slices were obtained using a confocal spinning-disk (CSU-X1; Yokogawa) upright microscope (DM6000FS; Leica) equipped with a ORCA Flash4.0LT camera (Hamamatsu) and a 25x 0.95NA W objective (Leica). All images were acquired with MetaMorph 7 imaging software (Molecular Devices) and analyzed with Image J homemade routines.

For the staining of BMDM, cells were fixed in PFA 4% immediately after the stimulation, permeabilized with frozen methanol 90%, stained overnight with pIRF3-AF647 or HDAC4 (abcam used at 1:100). For the detection of HDAC4, primary anti-HDAC4 Ab was revealed with an anti-rabbit Alexa 488 (life technologies; 1:200).

Images of BMDM were acquired on a wide-field Nikon Eclipse microscope through a 20x objective, with an Eclipse CCD camera (Photometrics). Due to the low labeling intensity, images of pIRF3 had to be acquired with a binning of 3, and 5 images were averaged. For the quantification of pIRF3 intensity, performed on images of BMDM, after background subtraction, the mean nuclear intensity was measured in 40-60 cells per condition. Images of HDAC were acquired without binning.

bioRxiv preprint doi: https://doi.org/10.1101/336990; this version posted July 9, 2019. The copyright holder for this preprint (which was not certified by peer review) is the author/funder. All rights reserved. No reuse allowed without permission.

Transcriptomic analysis

Tumor RNA was extracted using a RNeasy Mini Kit (Qiagen) according to the manufacturer's instructions. The RNA were reverse transcribed using the Advantage® RT for PCR kit (Applied Clontech) and gene expression was analyzed by RT-qPCR with the LighCycler® 480 Real-Time PCR system. The list of primers that were used is provided in the supplementary table 1.

ELISA

The IFNa production test was performed on entire tumor cell suspensions obtained after Ficoll density separation (Histopaque-1093 from Sigma) or after cell sorting and then stimulated overnight with 250 µg/ml of DMXAA. The ELISA test was performed using IFNa Mouse ELISA Kit (Thermo Fisher) according to the manufacturer's instructions.

Statistics

Data were analyzed with GraphPad Prism5 software to run unpaired Student's *t*-Test or One-way ANOVA and Tukey test for multiple comparison. For statistical analysis of in vivo treatments, the Kolmogorov-Smirnov test was run with Python software after estimation of the logarithmic fold-change $\log_{10}(V_{tumor}$ [5 days]$/V_{tumor}$[t=0]) of the mean tumor volume in individual mice between Day 0 and Day 5 after treatment initiation. Values ≤ 0.05 were considered significant. * $p<0.05$; ** $p<0.01$; *** $p<0.001$).

bioRxiv preprint doi: https://doi.org/10.1101/336990; this version posted July 9, 2019. The copyright holder for this preprint (which was not certified by peer review) is the author/funder. All rights reserved. No reuse allowed without permission.

References

1. Dunn, G. P. *et al.* A critical function for type I interferons in cancer immunoediting. *Nat. Immunol.* **6**, 722–729 (2005).
2. Diamond, M. S. *et al.* Type I interferon is selectively required by dendritic cells for immune rejection of tumors. *J. Exp. Med.* **208**, 1989–2003 (2011).
3. Fuertes, M. B. *et al.* Host type I IFN signals are required for antitumor CD8+ T cell responses through CD8α+ dendritic cells. *J. Exp. Med.* **208**, 2005–2016 (2011).
4. Hervas-Stubbs, S. *et al.* Direct Effects of Type I Interferons on Cells of the Immune System. *Clin. Cancer Res.* **17**, 2619–2627 (2011).
5. Santini, S. M. *et al.* Type I Interferon as a Powerful Adjuvant for Monocyte-Derived Dendritic Cell Development and Activity in Vitro and in Hu-Pbl-Scid Mice. *J. Exp. Med.* **191**, 1777–1788 (2000).
6. Kotredes, K. P. & Gamero, A. M. Interferons as inducers of apoptosis in malignant cells. *J. Interferon Cytokine Res. Off. J. Int. Soc. Interferon Cytokine Res.* **33**, 162–170 (2013).
7. Sujobert, P. & Trautmann, A. Conflicting Signals for Cancer Treatment. *Cancer Res.* **76**, 6768–6773 (2016).
8. Musella, M., Manic, G., De Maria, R., Vitale, I. & Sistigu, A. Type-I-interferons in infection and cancer: Unanticipated dynamics with therapeutic implications. *Oncoimmunology* **6**, (2017).
9. Woo, S.-R. *et al.* STING-Dependent Cytosolic DNA Sensing Mediates Innate Immune Recognition of Immunogenic Tumors. *Immunity* **41**, 830–842 (2014).
10. Corrales, L. *et al.* Direct Activation of STING in the Tumor Microenvironment Leads to Potent and Systemic Tumor Regression and Immunity. *Cell Rep.* **11**, 1018–1030 (2015).
11. Demaria, O. *et al.* STING activation of tumor endothelial cells initiates spontaneous and therapeutic antitumor immunity. *Proc. Natl. Acad. Sci. U. S. A.* **112**, 15408–15413 (2015).
12. Baguley, B. C. & Siemann, D. W. Temporal Aspects of the Action of ASA404 (Vadimezan; DMXAA). *Expert Opin. Investig. Drugs* **19**, 1413–1425 (2010).

bioRxiv preprint doi: https://doi.org/10.1101/336990; this version posted July 9, 2019. The copyright holder for this preprint (which was not certified by peer review) is the author/funder. All rights reserved. No reuse allowed without permission.

13. Jassar, A. S. *et al.* Activation of tumor-associated macrophages by the vascular disrupting agent 5,6-dimethylxanthenone-4-acetic acid induces an effective CD8+ T-cell-mediated antitumor immune response in murine models of lung cancer and mesothelioma. *Cancer Res.* **65**, 11752–11761 (2005).

14. Henare, K. *et al.* Dissection of stromal and cancer cell-derived signals in melanoma xenografts before and after treatment with DMXAA. *Br. J. Cancer* **106**, 1134–1147 (2012).

15. Fridlender, Z. G. *et al.* Using macrophage activation to augment immunotherapy of established tumours. *Br. J. Cancer* **108**, 1288–1297 (2013).

16. Weiss, J. M. *et al.* The STING agonist DMXAA triggers a cooperation between T lymphocytes and myeloid cells that leads to tumor regression. *Oncoimmunology* **6**, e1346765 (2017).

17. Joncker, N. T., Bettini, S., Boulet, D., Guiraud, M. & Guerder, S. The site of tumor development determines immunogenicity via temporal mobilization of antigen-laden dendritic cells in draining lymph nodes. *Eur. J. Immunol.* **46**, 609–618 (2016).

18. Wang, S.-F. *et al.* Early T Cell Signalling Is Reversibly Altered in PD-1+ T Lymphocytes Infiltrating Human Tumors. *PLoS ONE* **6**, e17621 (2011).

19. Franklin, R. A. *et al.* The cellular and molecular origin of tumor-associated macrophages. *Science* **344**, 921–925 (2014).

20. Zhang, Q. *et al.* Prognostic Significance of Tumor-Associated Macrophages in Solid Tumor: A Meta-Analysis of the Literature. *PLoS ONE* **7**, (2012).

21. Fridman, W. H., Zitvogel, L., Sautès-Fridman, C. & Kroemer, G. The immune contexture in cancer prognosis and treatment. *Nat. Rev. Clin. Oncol.* **14**, 717–734 (2017).

22. Beatty, G. L. *et al.* CD40 Agonists Alter Tumor Stroma and Show Efficacy Against Pancreatic Carcinoma in Mice and Humans. *Science* **331**, 1612–1616 (2011).

23. Klug, F. *et al.* Low-dose irradiation programs macrophage differentiation to an $iNOS^+$/M1 phenotype that orchestrates effective T cell immunotherapy. *Cancer Cell* **24**, 589–602 (2013).

bioRxiv preprint doi: https://doi.org/10.1101/336990; this version posted July 9, 2019. The copyright holder for this preprint (which was not certified by peer review) is the author/funder. All rights reserved. No reuse allowed without permission.

24. Ma, Y. *et al.* Anticancer Chemotherapy-Induced Intratumoral Recruitment and Differentiation of Antigen-Presenting Cells. *Immunity* **38**, 729–741 (2013).

25. Thoreau, M. *et al.* Vaccine-induced tumor regression requires a dynamic cooperation between T cells and myeloid cells at the tumor site. *Oncotarget* **6**, 27832–27846 (2015).

26. Sektioglu, I. M. *et al.* Macrophage-derived nitric oxide initiates T-cell diapedesis and tumor rejection. *Oncoimmunology* **5**, e1204506 (2016).

27. Burdette, D. L. & Vance, R. E. STING and the innate immune response to nucleic acids in the cytosol. *Nat. Immunol.* **14**, 19–26 (2013).

28. Roberts, Z. J. *et al.* The chemotherapeutic agent DMXAA potently and specifically activates the TBK1-IRF-3 signaling axis. *J. Exp. Med.* **204**, 1559–1569 (2007).

29. Zhang, F. *et al.* TGF-β induces M2-like macrophage polarization via SNAIL-mediated suppression of a pro-inflammatory phenotype. *Oncotarget* **7**, 52294–52306 (2016).

30. Wang, L.-C. S. *et al.* Neutrophil influx and chemokine production during the early phases of the antitumor response to the vascular disrupting agent DMXAA (ASA404). *Neoplasia N. Y. N* **11**, 793–803 (2009).

31. Yang, Q. *et al.* Host HDAC4 Regulates the Antiviral Response by Inhibiting the Phosphorylation of IRF3. *J. Mol. Cell Biol.* (2018). doi:10.1093/jmcb/mjy035

32. Guo, W. *et al.* TGF-β1 stimulates HDAC4 nucleus-to-cytoplasm translocation and NADPH oxidase 4-derived reactive oxygen species in normal human lung fibroblasts. *Am. J. Physiol. Lung Cell. Mol. Physiol.* **312**, L936–L944 (2017).

33. Critchley-Thorne, R. J. *et al.* Impaired interferon signaling is a common immune defect in human cancer. *Proc. Natl. Acad. Sci. U. S. A.* **106**, 9010–9015 (2009).

34. Ng, K. W., Marshall, E. A., Bell, J. C. & Lam, W. L. cGAS-STING and Cancer: Dichotomous Roles in Tumor Immunity and Development. *Trends Immunol.* **39**, 44–54 (2018).

bioRxiv preprint doi: https://doi.org/10.1101/336990; this version posted July 9, 2019. The copyright holder for this preprint (which was not certified by peer review) is the author/funder. All rights reserved. No reuse allowed without permission.

35. Xia, T., Konno, H. & Barber, G. N. Recurrent Loss of STING Signaling in Melanoma Correlates with Susceptibility to Viral Oncolysis. *Cancer Res.* **76**, 6747–6759 (2016).

36. Moses, H. & Barcellos-Hoff, M. H. TGF-β Biology in Mammary Development and Breast Cancer. *Cold Spring Harb. Perspect. Biol.* **3**, (2011).

37. Lin, R.-L. & Zhao, L.-J. Mechanistic basis and clinical relevance of the role of transforming growth factor-β in cancer. *Cancer Biol. Med.* **12**, 385–393 (2015).

38. Chen, Y. *et al.* High p-Smad2 expression in stromal fibroblasts predicts poor survival in patients with clinical stage I to IIIA non-small cell lung cancer. *World J. Surg. Oncol.* **12**, (2014).

39. Mantovani, A., Sozzani, S., Locati, M., Allavena, P. & Sica, A. Macrophage polarization: tumor-associated macrophages as a paradigm for polarized M2 mononuclear phagocytes. *Trends Immunol.* **23**, 549–555 (2002).

40. Chen, W., Frank, M. E., Jin, W. & Wahl, S. M. TGF-beta released by apoptotic T cells contributes to an immunosuppressive milieu. *Immunity* **14**, 715–725 (2001).

41. Sugiyama, Y. *et al.* Smad2 and Smad3 are redundantly essential for the suppression of iNOS synthesis in macrophages by regulating IRF3 and STAT1 pathways. *Int. Immunol.* **24**, 253–265 (2012).

42. Sisirak, V. *et al.* Breast cancer-derived transforming growth factor-β and tumor necrosis factor-α compromise interferon-α production by tumor-associated plasmacytoid dendritic cells. *Int. J. Cancer* **133**, 771–778 (2013).

43. Fridlender, Z. G. *et al.* Polarization of tumor-associated neutrophil phenotype by TGF-beta: 'N1' versus 'N2' TAN. *Cancer Cell* **16**, 183–194 (2009).

44. Esquerré, M. *et al.* Human regulatory T cells inhibit polarization of T helper cells toward antigen-presenting cells via a TGF-beta-dependent mechanism. *Proc. Natl. Acad. Sci. U. S. A.* **105**, 2550–2555 (2008).

bioRxiv preprint doi: https://doi.org/10.1101/336990; this version posted July 9, 2019. The copyright holder for this preprint (which was not certified by peer review) is the author/funder. All rights reserved. No reuse allowed without permission.

45. Takaku, S. *et al.* Blockade of TGF-β enhances tumor vaccine efficacy mediated by CD8+ T cells. *Int. J. Cancer J. Int. Cancer* **126**, 1666 (2010).

46. Sarkar, A., Donkor, M. K. & Li, M. O. T cell- but not tumor cell-produced TGF-β1 promotes the development of spontaneous mammary cancer. *Oncotarget* **2**, 1339–1351 (2011).

47. Mariathasan, S. *et al.* TGFβ attenuates tumour response to PD-L1 blockade by contributing to exclusion of T cells. *Nature* **554**, 544–548 (2018).

48. Tauriello, D. V. F. *et al.* TGFβ drives immune evasion in genetically reconstituted colon cancer metastasis. *Nature* **554**, 538–543 (2018).

49. Spaapen, R. M. *et al.* Therapeutic activity of high-dose intratumoral IFN-β requires direct effect on the tumor vasculature. *J. Immunol. Baltim. Md 1950* **193**, 4254–4260 (2014).

50. Sistigu, A. *et al.* Cancer cell-autonomous contribution of type I interferon signaling to the efficacy of chemotherapy. *Nat. Med.* **20**, 1301–1309 (2014).

51. Bougherara, H. *et al.* Real-Time Imaging of Resident T Cells in Human Lung and Ovarian Carcinomas Reveals How Different Tumor Microenvironments Control T Lymphocyte Migration. *Front. Immunol.* **6**, 500 (2015).

bioRxiv preprint doi: https://doi.org/10.1101/336990; this version posted July 9, 2019. The copyright holder for this preprint (which was not certified by peer review) is the author/funder. All rights reserved. No reuse allowed without permission.

Acknowledgements:

We are really grateful to C. Kantari Mimoun for her critical review of the manuscript, and the staff of the IMAG'IC, CYBIO and GENOM'IC facilities of the Cochin Institute for their advice all along this study.

Author contributions:

M.G. and N.B. designed the experiments, M.G., F.R., V.F., L.V., J.M.W., M.T. G.B. and N.B. performed and analyzed the experiments, T.G. helped with image analysis with Image J. N.B. and A.T. designed the study and M.G., A.T and N.B. wrote the manuscript and prepared the figures.

Funding support:

This work was granted by Worldwide Cancer Research (UK), the "Comité de Paris de La Ligue Contre le Cancer", the Cancer Research for Personalized Medicine (CARPEM), Plan Cancer (Tumor Heterogeneity and Ecosystem Program), the CNRS, INSERM and University Paris-Descartes. M. G. was granted by the Ministère de l'Education Nationale, de l'Enseignement Supérieur et de la Recherche.

Conflict of interests statement: The authors have declared that no conflict of interest exists

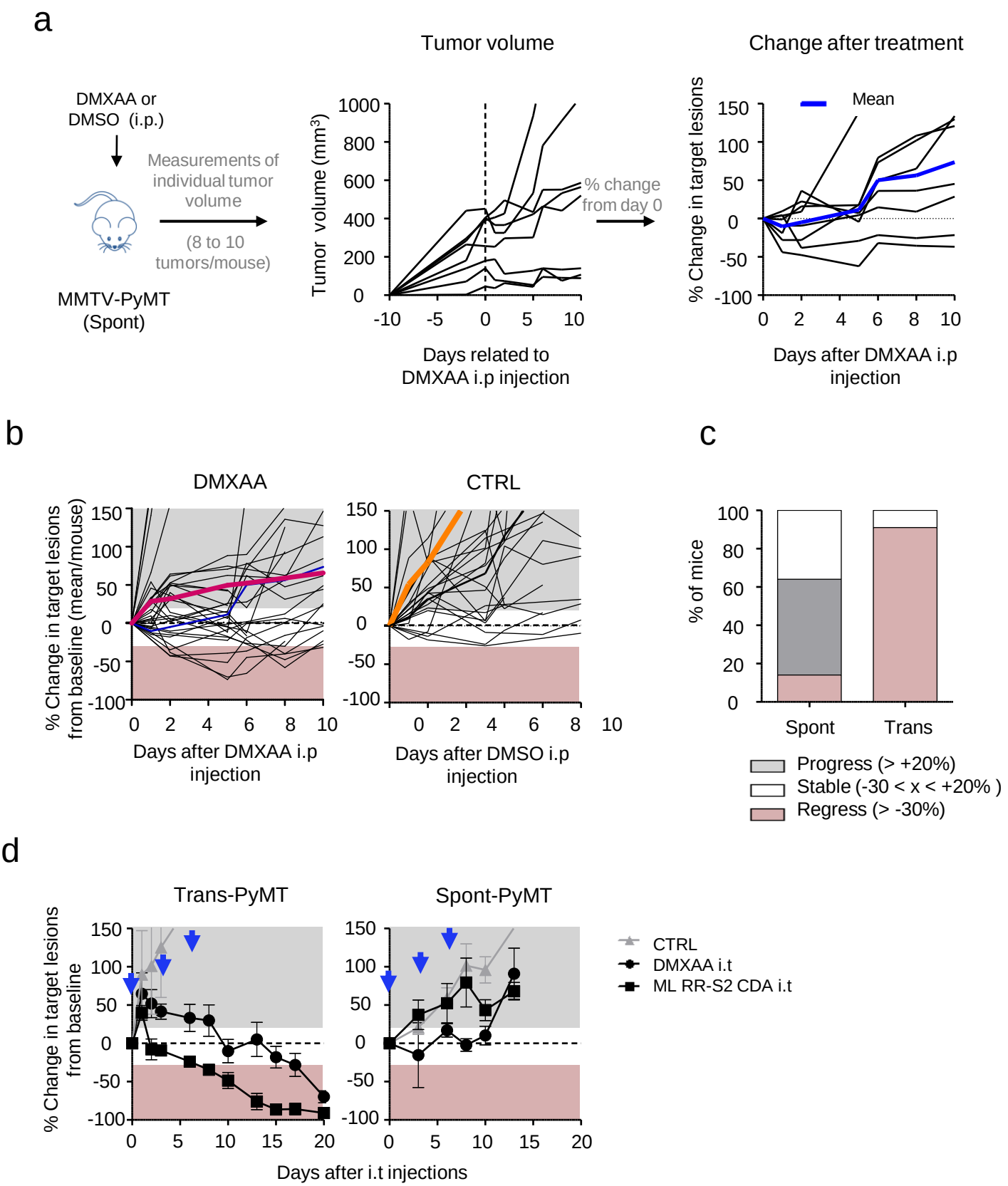
a
DMXAA or
DMSO (i.p.)
Measurements of
individual tumor
volume
(8 to 10
tumors/mouse)
MMTV-PyMT
(Spont)
Tumor volume
Tumor volume (mm3)
1000
800
600
400
200
0
-10
-5
0
5
10
Days related to
DMXAA i.p injection
% change
from day 0
Change after treatment
% Change in target lesions
150
100
50
0
-50
-100
Mean
0
2
4
6
8
10
Days after DMXAA i.p
injection
b
DMXAA
CTRL
% Change in target lesions
from baseline (mean/mouse)
Days after DMXAA i.p
injection
Days after DMSO i.p
injection
c
% of mice
100
80
60
40
20
0
Spont
Trans
Progress (> +20%)
Stable (-30 < x < +20%)
Regress (> -30%)
d
Trans-PyMT
Spont-PyMT
% Change in target lesions
from baseline
0
5
10
15
20
Days after i.t injections
CTRL
DMXAA i.t
ML RR-S2 CDA i.t

Fig 1

bioRxiv preprint doi: https://doi.org/10.1101/336990; this version posted July 9, 2019. The copyright holder for this preprint (which was not certified by peer review) is the author/funder. All rights reserved. No reuse allowed without permission.

Figure 1. DMXAA does not induce a systematic regression of Spont-PyMT tumors. (a) Spont-PyMT mice were treated at day 0 with one i.p. injection of DMXAA or DMSO as control. For each treated mouse, the changes in tumor size from baseline (d0) was calculated at each time point and expressed relative to the size at d0. The graphs in (a) provide an example of measurements obtained in one mouse treated with DMXAA i.p., with one curve per tumor. The average curve of all tumors of this mouse is shown in blue. **(b)** Each black curve corresponds to one mouse, and is calculated as the average relative tumor changes for this mouse (as shown in a). The average curves for all the animals of a cohort are shown in red (DMXAA) or orange (CTRL). **(c)** The proportion of mice with, on average, regressing, stabilized or progressing tumors, are represented for these Spont-PyMT mice, in comparison to Trans-PyMT mice. Spont-PyMT mice: *n*= 30; Trans-PyMT mice: *n*= 26, from 9 to 10 independent experiments. **(d)** Intratumoral injection of DMXAA or ML RR-S2 CDA induced tumor regression in Trans-PyMT mice, but not in Spont-PyMT mice. Trans- and Spont-PyMT mice were injected i.t. with DMXAA (1x 500 µg) or ML RR-S2 (3x50 µg) at days 0, 3 and 6 (black arrows) or with HBSS i.t. as controls. The average fold change in tumor volume compared to baseline (day 0) is shown for each treated group. ML RR-S2 group (n=3 to 10 mice), DMXAA (n=3 to 10 mice) and HBSS (n=4 to 6 mice). Data are from 3 independent experiments.

a

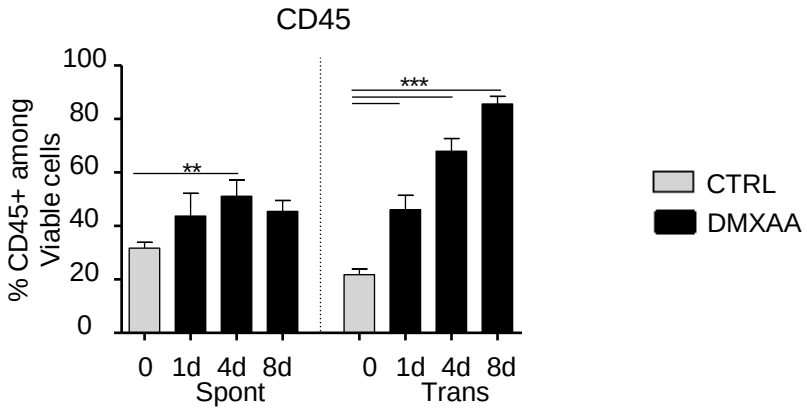
CD45
% CD45+ among Viable cells
100
80
60
40
20
0
**
***
0 1d 4d 8d
Spont
0 1d 4d 8d
Trans
CTRL
DMXAA

b

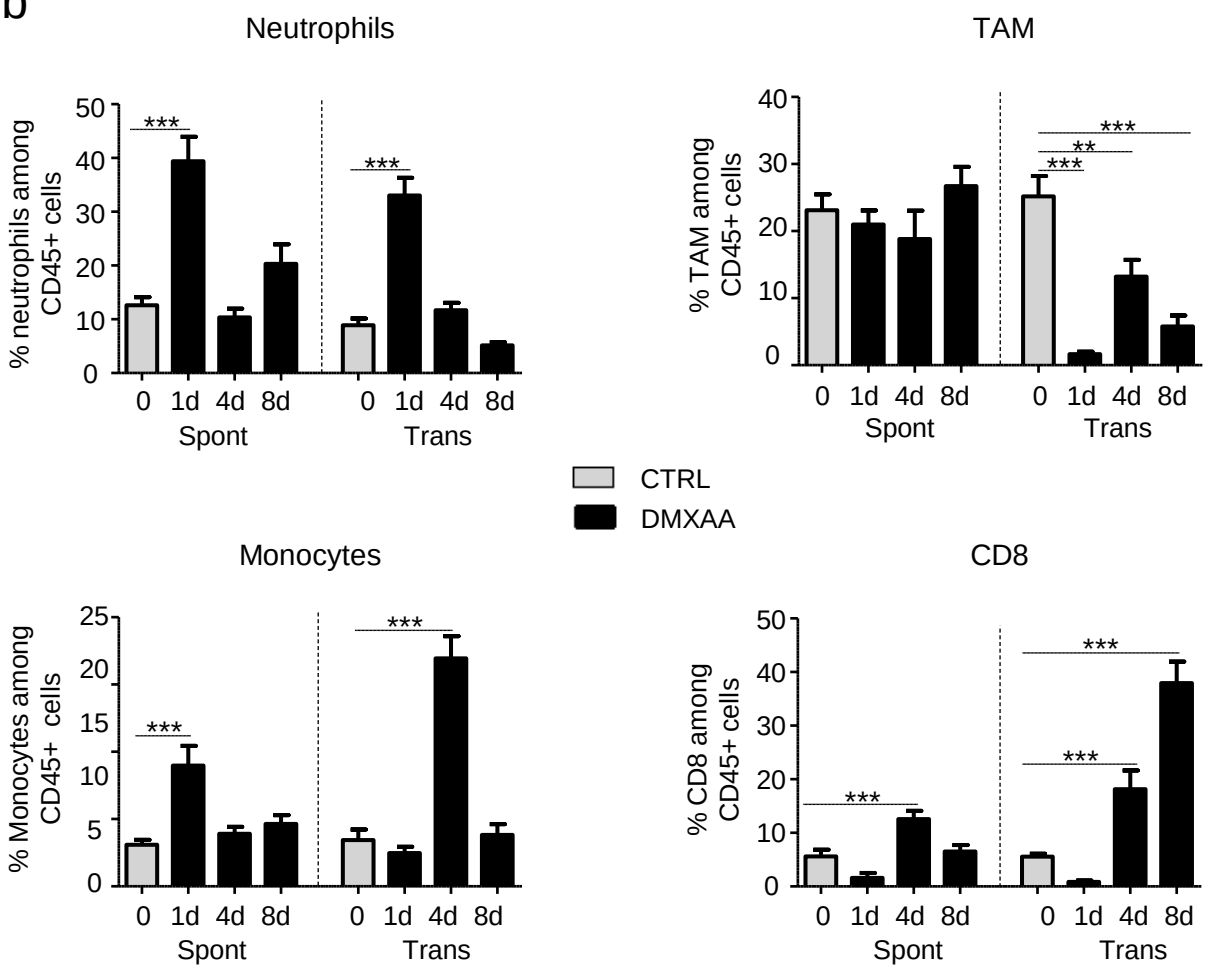
Neutrophils
% neutrophils among CD45+ cells
50
40
30
20
10
0
***
***
0 1d 4d 8d
Spont
0 1d 4d 8d
Trans
TAM
% TAM among CD45+ cells
40
30
20
10
0
***
**
***
0 1d 4d 8d
Spont
0 1d 4d 8d
Trans
CTRL
DMXAA
Monocytes
% Monocytes among CD45+ cells
25
20
15
10
5
0
***
***
0 1d 4d 8d
Spont
0 1d 4d 8d
Trans
CD8
% CD8 among CD45+ cells
50
40
30
20
10
0
***
***
***
0 1d 4d 8d
Spont
0 1d 4d 8d
Trans

Fig 2

bioRxiv preprint doi: https://doi.org/10.1101/336990; this version posted July 9, 2019. The copyright holder for this preprint (which was not certified by peer review) is the author/funder. All rights reserved. No reuse allowed without permission.

Figure 2. DMXAA induces a weak immune infiltrate in Spont-PyMT tumors. (a) The proportion of $CD45^+$ cells in Spont-PyMT or Trans-PyMT tumors before treatment (grey bars) and at days 1 to 8 after DMXAA i.p. injection (black bars) was determined by flow cytometry after dissociation of the tumors. **(b)** The proportion of neutrophils, TAM, monocytes and $CD8^+$ T cells among those $CD45^+$ cells are shown. Spont-PyMT mice: *n*= 4-12; Trans-PyMT mice: *n*= 10-30. Data are from 3-7 independent experiments for each group of mice. Results are expressed as mean ± s.e.m. Tukey's Multiple Comparison Test.

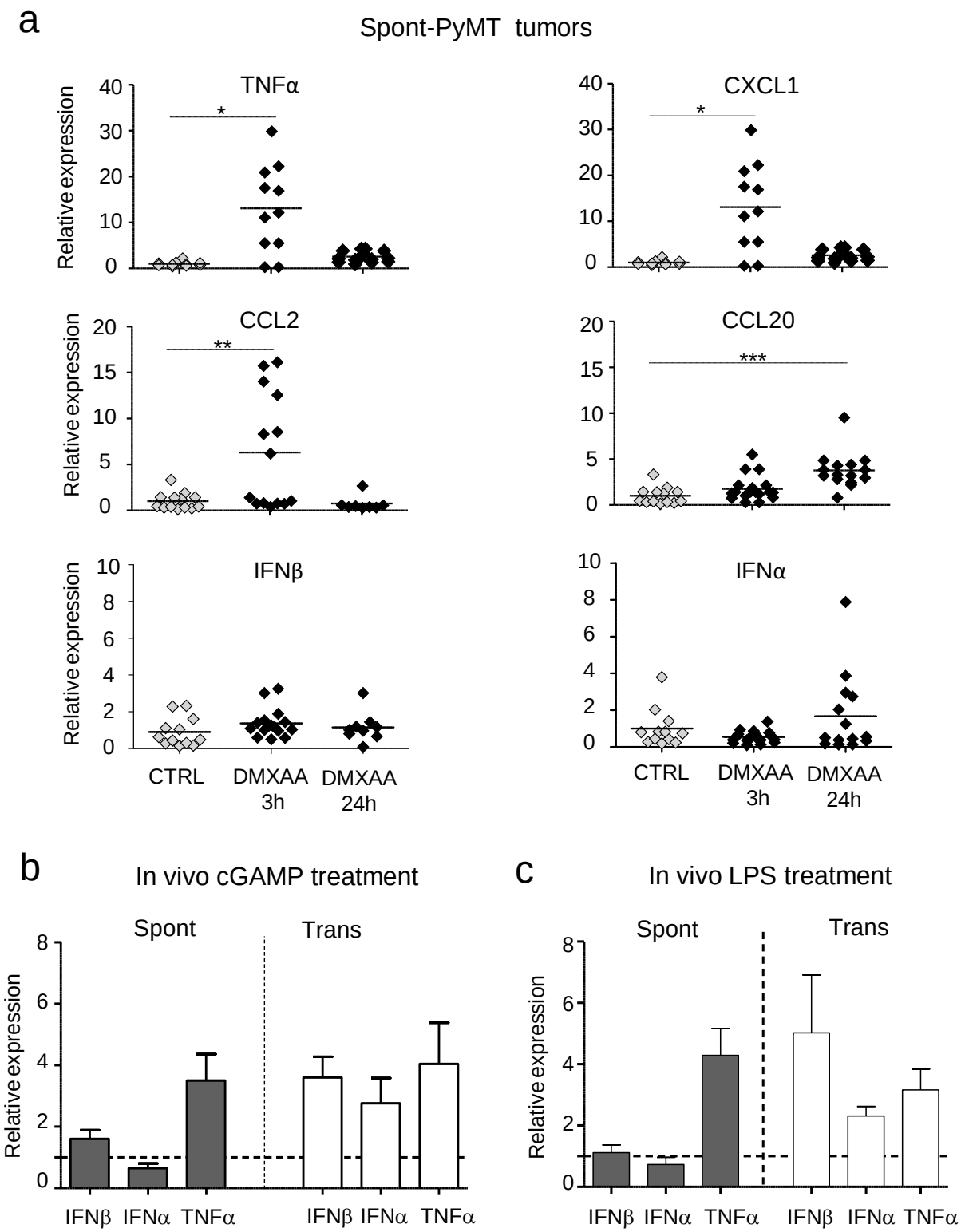
a
Spont-PyMT tumors
TNFα
CXCL1
CCL2
CCL20
IFNβ
IFNα
Relative expression
CTRL
DMXAA 3h
DMXAA 24h
b
In vivo cGAMP treatment
Spont
Trans
IFNβ IFNα TNFα
c
In vivo LPS treatment

Fig 3

bioRxiv preprint doi: https://doi.org/10.1101/336990; this version posted July 9, 2019. The copyright holder for this preprint (which was not certified by peer review) is the author/funder. All rights reserved. No reuse allowed without permission.

Figure 3. Lack of type I IFN triggering in Spont-PyMT tumors. (a) Spont-PyMT mice were injected i.p. with DMXAA and then sacrificed after 3 hours and 24 hours to measure mRNA levels of cytokines and chemokines in tumors. The relative expressions compared to DMSO treated mice are shown. Each dot corresponds to one tumor. Cumulative data from CTRL: *n*=6 mice and DMXAA: *n*=6 mice, from 3 independent experiments, are shown. Tukey's Multiple Comparison Test. **(b and c)** The relative expression of these cytokines/chemokines, compared to PBS (CTRL) injected mice, were measured in Spont-PyMT and Trans-PyMT target lesion 3 hours after **(b)** cGAMP (25μg i.t.) injection (Spont-PyMT mice: *n*= 3 CTRL and *n*=3 cGAMP; Trans-PyMT mice: *n*= 5 CTRL and *n*=13 cGAMP) or **(c)** LPS (50μg i.p.) injection (Spont-PyMT mice: *n*= 3 CTRL and *n*=3 LPS; Trans-PyMT mice: *n*= 5 CTRL and *n*=10 LPS). In **b** and **c**, results are expressed as mean ± s.e.m.

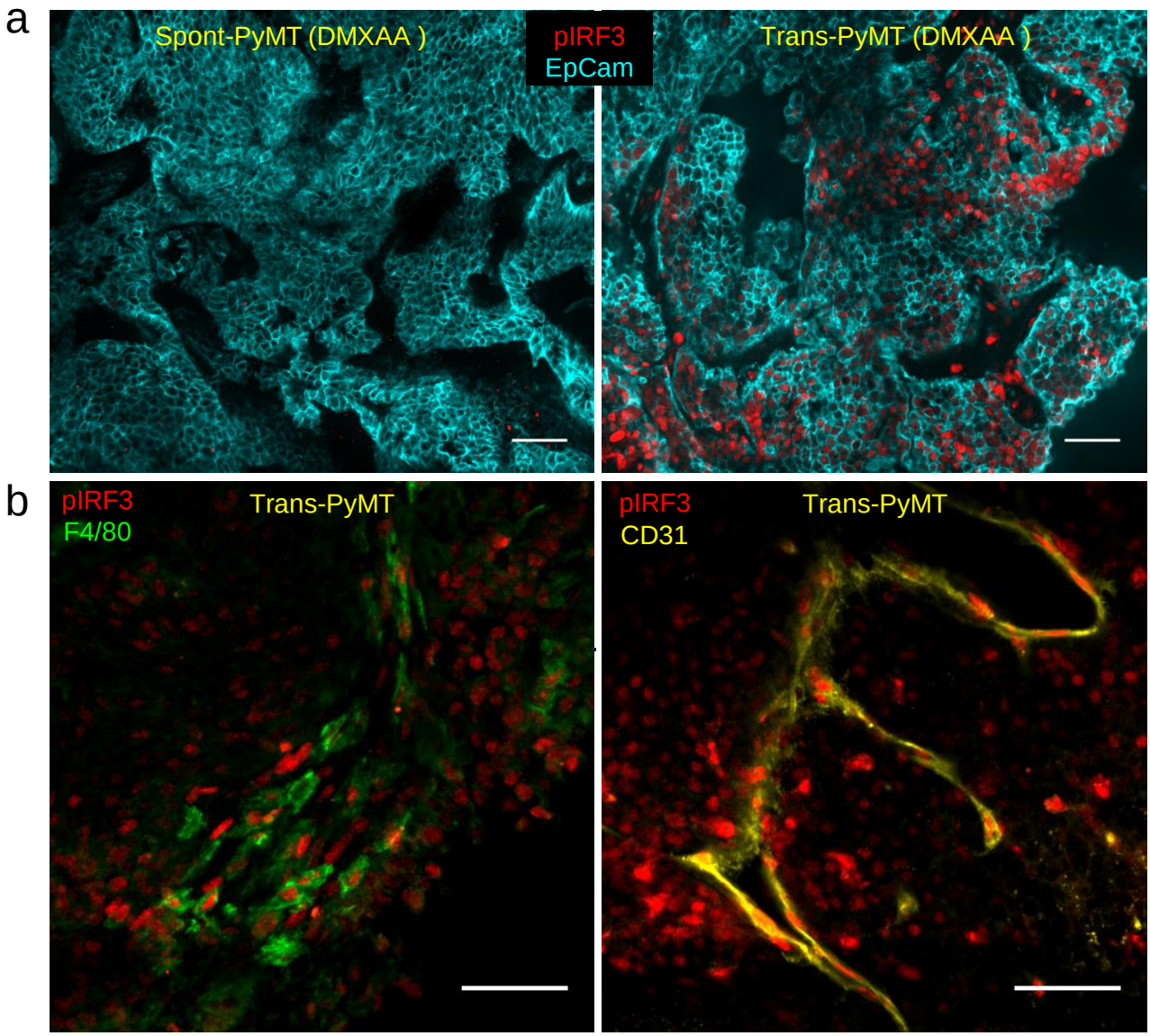
a
Spont-PyMT (DMXAA)
pIRF3
EpCam
Trans-PyMT (DMXAA)
b
pIRF3
F4/80
Trans-PyMT
pIRF3
CD31
Trans-PyMT

Fig 4

bioRxiv preprint doi: https://doi.org/10.1101/336990; this version posted July 9, 2019. The copyright holder for this preprint (which was not certified by peer review) is the author/funder. All rights reserved. No reuse allowed without permission.

Figure 4. Absence of IRF3 phosphorylation in Spont-PyMT tumors, compared to Trans-PyMT tumors, after DMXAA injection. (a) Spont-PyMT mice and Trans-PyMT mice received one i.p. injection of DMXAA. Three hours later, tumors were collected and tumors slices were stained with anti-EpCAM (blue) and anti-pIRF3 (red) mAbs. Representative images from Spont-PyMT tumors (left) and Trans-PyMT tumors (right) are shown. **(b)** In Trans-PyMT tumors, some pIRF3^{+} cells (red) are myeloid (F4/80^{+}, green), or endothelial cells (CD31^{+}, yellow). Scale bars = 50 µm. Data are representative of 3 Spont-PyMT and 5 Trans-PyMT mice, from 5 independent experiments.

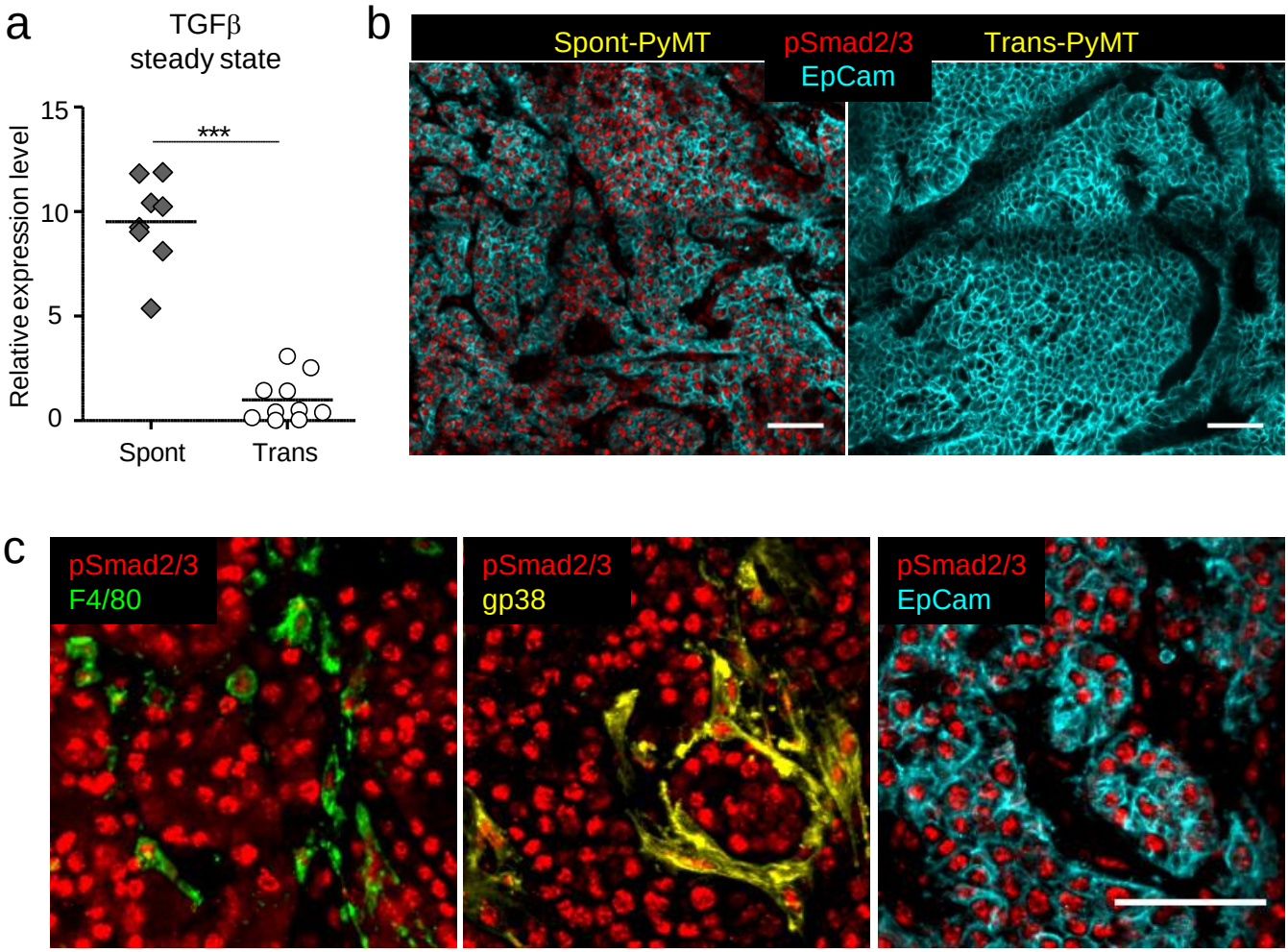
a
TGFβ
steady state
Relative expression level
15
10
5
0
***
Spont
Trans
b
Spont-PyMT
pSmad2/3
EpCam
Trans-PyMT
c
pSmad2/3
F4/80
pSmad2/3
gp38
pSmad2/3
EpCam

Fig 5

bioRxiv preprint doi: https://doi.org/10.1101/336990; this version posted July 9, 2019. The copyright holder for this preprint (which was not certified by peer review) is the author/funder. All rights reserved. No reuse allowed without permission.

Figure 5. The expression of TGFβ in Spont-PyMT is associated with phosphorylation of Smad2/3 in tumor and infiltrating cells. (a) mRNA levels of *Tgfβ* were measured in untreated Spont- and Trans-PyMT tumors, right after tumor dissociation. The relative expression, normalized to Trans-PyMT tumors is shown. Each dot corresponds to one tumor. Cumulative data from Trans-PyMT mice: *n*=10 and Spont-PyMT mice: *n*=3. Student *t*-Test. **(b)** Tumors slices from Spont- and Trans-PyMT untreated mice, were stained with anti-EpCAM (blue) and anti-pSmad2/3 (red) Abs. **(c)** In Spont-PyMT tumors, pSmad2/3 $^{+}$ cells (red) may be myeloid cells (F4/80^{+}, green), fibroblasts (gp38^{+}, yellow) or tumor cells (EpCAM^{+}, cyan). Note that the 2nd and 3rd images, not superimposed for clarity, are from the same image field. Images are representative of Spont-PyMT: *n*= 3 mice; Trans-PyMT: *n*= 3 mice, from 3 independent experiments for each group of mice. In b and c, scale bars = 50 µm.

a

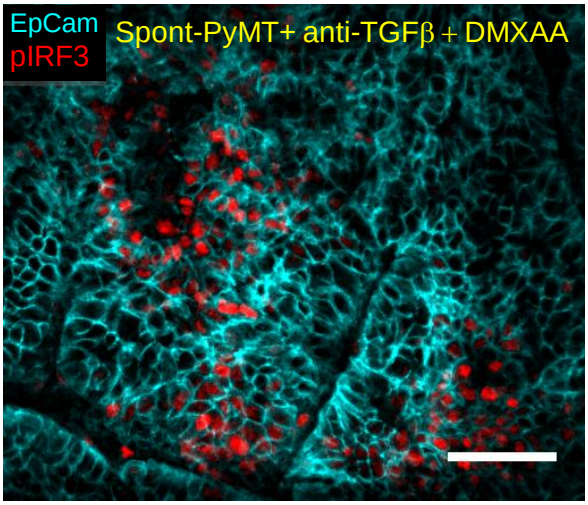
EpCam
pIRF3
Spont-PyMT+ anti-TGFβ + DMXAA

b

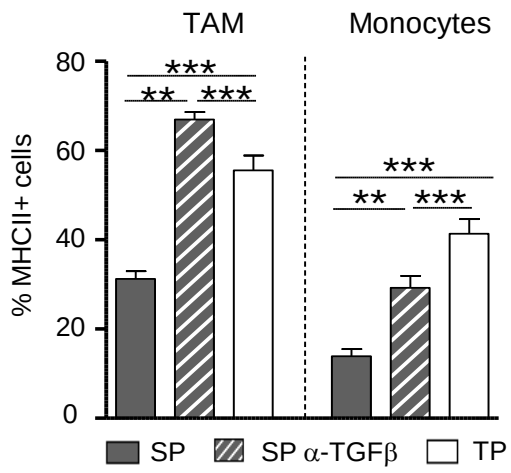
TAM
Monocytes
% MHCII+ cells
80
60
40
20
0
***
**
***
***
**
***
SP
SP α-TGFβ
TP

c

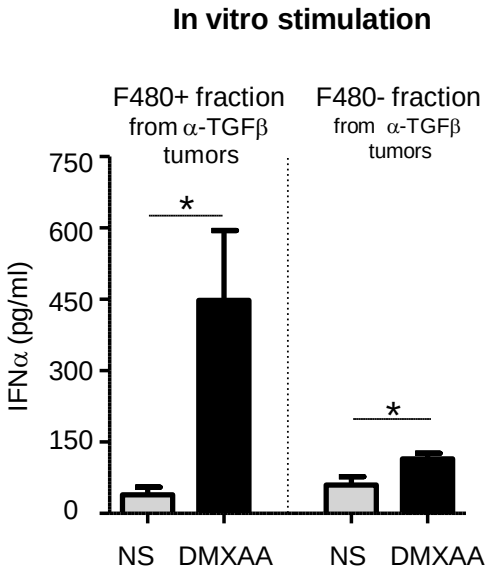
In vitro stimulation
F480+ fraction from α-TGFβ tumors
F480- fraction from α-TGFβ tumors
IFNα (pg/ml)
750
600
450
300
150
0
*
*
NS
DMXAA
NS
DMXAA

d

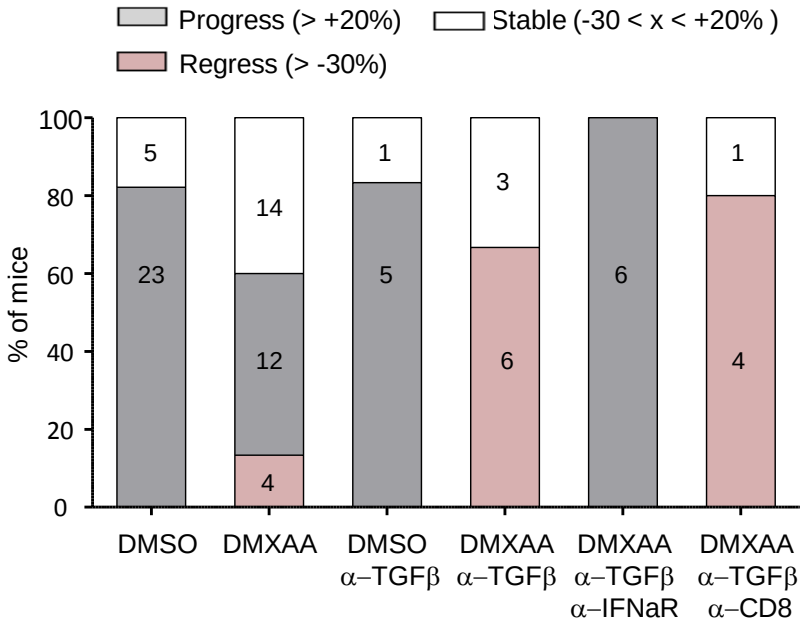
Progress (> +20%)
Stable (-30 < x < +20%)
Regress (> -30%)
% of mice
100
80
60
40
20
0
5
23
14
12
4
1
5
3
6
6
1
4
DMSO
DMXAA
DMSO α–TGFβ
DMXAA α–TGFβ
DMXAA α–TGFβ α–IFNaR
DMXAA α–TGFβ α–CD8

Fig 6

bioRxiv preprint doi: https://doi.org/10.1101/336990; this version posted July 9, 2019. The copyright holder for this preprint (which was not certified by peer review) is the author/funder. All rights reserved. No reuse allowed without permission.

Figure 6. Blocking TGFβ allows DMXAA-induced type I IFN production and the regression of Spont-PyMT tumors. (a) Spont-PyMT mice, treated with an anti-TGFβ (day-4 and day-1), received one i.p. injection of DMXAA. Three hours later, tumors were collected and tumor slices were stained with anti-EpCAM (blue) and anti-pIRF3 (red) mAbs. The image is representative of *n*=4 anti-TGFβ-treated Spont-PyMT mice. **(b)** Tumors from Spont-PyMT mice, treated or not anti-TGFβ Ab, and from Trans-PyMT mice, were analyzed by flow cytometry for the expression of MHC class II on TAM and Monocytes. Data are from anti-TGFβ treated Spont-PyMT mice: *n*=7; Spont-PyMT mice: *n*=6-8; Trans-PyMT mice: *n*=12-21, collected in 7 independent experiments. Results are expressed as mean ± s.e.m. Tukey's Multiple Comparison Test**. (c)** Tumors from anti-TGFβ treated Spont-PyMT mice were collected and pooled for each mouse (8-10 tumors), and dissociated. The cell suspensions were enriched in immune cells before F4/80^{+} cells were sorted with magnetic beads. F4/80^{+} and F4/80^{-} cells were restimulated *in vitro* with DMXAA (250µg/ml) and IFNα was measured by ELISA in the supernatant after overnight culture. Results are expressed as mean ± s.e.m. Student *t*-Test. **(d)** Spont-PyMT mice were treated with DMXAA (i.p. at day 0) or DMSO as control, with anti-TGFβ (i.p. 200ug), anti-IFNAR (i.p. 200ug) and /or with anti-CD8 (i.p. 200ug) Abs on day-4, day-1, day1, day4. The proportion of mice with an average regressing, stabilized or progressing tumors, are shown as in Figure 1. DMSO treated mice: *n*=28; DMXAA treated mice: *n*=30; DMSO + anti-TGFβ: *n*=6; DMXAA + anti-TGFβ: *n*=9; DMXAA + anti-TGFβ + anti-IFNAR: *n*=6; DMXAA + anti-TGFβ + anti-CD8: *n*=5. Statistics are shown in supplementary Table 2.